Conference Paper, Published Version

Zinke, Peggy

Flow resistance parameters for natural emergent vegetation derived from a porous media model

River Flow 2010 - Dittrich, Koll, Aberle & Geisenhainer (eds) - © 2010 Bundesanstalt für Wasserbau ISBN 978-3-939230-00-7

Flow resistance parameters for natural emergent vegetation derived from a porous media model

Peggy Zinke
Institute for Water and Environmental Engineering, Norwegian University of Science and Technology, Trondheim, Norway

ABSTRACT: Methods from porous flow were adapted to compute the pore friction coefficient f_P and the pore Reynolds number Re_P for emergent natural vegetation based on criteria such as biomass and leaf area index. The calculated relations between f_P and Re_P for a limited number of flume and field data sets were shown in a Moody chart. There was an apparent scatter, but most of the data points of the investigated data sets were concentrated within a belt above a curve which was published for packed beds of various porous media. The investigation showed that it is necessary to have sufficient information about the vertical structure of the vegetation to characterize its flow resistance. For the sedge type, it was shown that the projected area changed significantly with height, but the spacing between the leaves did not. This is assumed to affect turbulence and to have a "laminarising" effect on the flow inside the vegetation. More data sets have to be included to test and develop the approach.

Keywords: Flow resistance, Vegetation, Wetlands, Porous flow

1 INTRODUCTION

The hydrological conditions of natural wetlands are characterized by shallow water depths and low flow velocities during the most periods of the year. Together with the influence of the vegetation on the flow, this implicates transitional or laminar flow conditions (Kadlec 1990, Tsihrintzis and Madiedo 2000, Serra et al. 2004). The fluid friction, however, is mostly computed from drag on single objects according to classical flow theory past immersed bodies, since the stems are typically spaced many diameters apart. For an array consisting of many elements, the flow resistance is often represented as volume-averaged drag force:

$$F_D = \frac{1}{2} \rho \, C_D \, a \, U_0^2 \qquad (1)$$

where F_D is the drag force; ρ the density of water; C_D is the bulk drag coefficient; a is the average vegetation density; and U_0 is the average (macroscopic) flow velocity.

According to this approach, vegetation with simple stem morphology can be sufficiently characterized by an average vegetation density a which is the frontal area of vegetation per unit volume and calculated as the product of the stem or blade width, d, and the number of stems per bed area, m. The drag coefficient C_D is expected to range between 1.0 and 1.2 for a single stiff cylinder with a stem Reynolds number $Re_d = Ud/\nu$ between 10^3 and 10^5 (ν = kinematic viscosity). It is different for other shapes, and it is higher under transitional flow conditions with lower Re_d (Douglas et al. 2005). The effect of wake sheltering in high stem densities is taken into account by reducing the bulk drag coefficient (Lindner 1982, Nepf 1999).

In some cases, flow inside vegetation has been successfully treated as porous flow (Ivanov 1975, Hoffmann 2004).

However, a general description of the flow resistance of emergent vegetation that is not focused on the stiff-cylinder analogy, but is based on parameters for real vegetation which can be easily measured, is still missing. The objective of this paper is therefore to investigate whether the flow resistance of emergent wetland vegetation can be described and compared using parameters like biomass or leaf area index together with the porous media flow concept. Special attention is paid to the vertical structure of the vegetation and its influence on flow resistance and turbulence.

2 THEORETICAL BACKGROUND

2.1 *Equations and definitions for porous media*

For a single-phase flow through a porous medium and low Reynolds numbers, Darcy stated that the superficial or macroscopic velocity U_0 is proportional to the pressure gradient $\Delta P/H$

$$U_0 = -\frac{K}{\mu}\frac{\Delta P}{H} \tag{2}$$

where K is the permeability of the porous medium and μ the dynamic viscosity. The permeability depends only on the material structure of the porous media and not on the properties of the fluid. It is related to the hydraulic conductivity (filtration coefficient) k_f according to:

$$k_f = \frac{g\rho K}{\mu} = \frac{gK}{\upsilon} \tag{3}$$

where g is the gravitational acceleration and ρ the fluid density. At higher Re, inertia forces increase and cannot be neglected anymore. The drag of the porous medium can be described by adding a non-linear term, leading to the Forchheimer equation:

$$-\frac{\Delta P}{H} = \frac{\mu U_0}{K} + b\rho U_o^{\,2} \tag{4}$$

where b is an empirical coefficient. Analogue expressions can be derived for 3D flow. The permeability and the Forchheimer tensor can be computed from the mean particle diameter of the solid obstacles and the porosity of the porous medium, for example using the modified Ergun equation (Breugem 2004).

It has been shown that Darcy's Law and the Forchheimer equation can be obtained from applying the volume-averaging technique for the microscopic flow to the Navier-Stokes equations (Whitaker 1996).

It is possible to represent a porous medium as a bundle of identical cylindrical tortuous pores characterized by a characteristic pore diameter d_P and a tortuosity T. Following Comiti and Renaud (1989), the pore diameter d_P and the pore or microscopic velocity U_P can be defined by:

$$d_P = \frac{4\varepsilon}{(1-\varepsilon)a_{vd}} \tag{5}$$

$$U_P = U_0\frac{T}{\varepsilon} \tag{6}$$

where ε is the porosity and a_{vd} the dynamic specific surface area. Here the dynamic surface area is defined as the ratio of the surface area actually presented by the particle to the flow to the volume of the solid. Introduced for the case of densely packed beds of flat plates, it is intended to account for the possibility of partial mutual overlapping of the particles, which produces a reduction in surface area compared to the "static" mean surface area of all particles.

The tortuosity T serves as geometric relation between the superficial velocity and the average stream-wise velocity in the pore channels. It was shown by Diedericks and Du Plessis (1997) that the tortuosity in anisotropic materials differs with direction of flow. According to Hoffmann (2004), the tortuosity in stream-wise direction for an anisotropic porous medium consisting of erected stiff cylinders can be expressed by:

$$T = \frac{\varepsilon}{1-\sqrt{(1-\varepsilon)}(4/\pi)} \tag{7}$$

From the capillary-type representation, one can define two characteristic dimensionless numbers by analogy with those corresponding to steady and uniform flow through a circular pipe (Douglas et al. 2005, Comiti et al. 2000): the pore friction factor f_P and the pore Reynolds number Re_P

$$f_p = \frac{\Delta P}{L}\frac{d_P}{4}\frac{1}{(1/2\rho U_P^2)} = \frac{\Delta P}{H}\frac{2\varepsilon^3}{T^3\rho(1-\varepsilon)a_{vd}U_0^2} \tag{8}$$

$$\mathrm{Re}_P = \frac{U_P d_P}{\upsilon} = \frac{4U_0 T}{\upsilon\, a_{vd}(1-\varepsilon)} \tag{9}$$

where L is the equivalent pore length. For a flow driven by the bed slope gradient, f_P is related to the canopy drag $C_D\,a$ in Equation 1 via:

$$C_D a = \frac{T^3(1-\varepsilon)\; a_{vd} f_P}{\varepsilon^2} \tag{10}$$

Comiti et al. (2000) found from experimental data for flow through packed beds of various porous media the following relation:

$$f_P = \frac{16}{\mathrm{Re}_P} + 0.194 \tag{11}$$

They noted that Re_P was the most appropriate parameter to characterize the flow even for the assumed limit of the capillary model in highly porous reticulated media. The idea that a Reynolds number based on inter-cylinder or inter-fibre spacing is the most relevant parameter in dilute arrays was also supported by Koch and Ladd (1997).

2.2 *Vegetation parameters for porous flow*

According to Equation 8 and 9 one needs three properties of the porous media to characterize its flow resistance: the porosity ε, the dynamic spe-

cific surface area a_{vd}, and the tortuosity T. The porosity of vegetation is defined as

$$\varepsilon = \frac{V - V_P}{V} \tag{12}$$

where V is the control volume and V_P the total volume of the plants in V. The relation

$$\phi = \frac{V_P}{V} = 1 - \varepsilon \tag{13}$$

is the solid volume fraction. V_P can be easily estimated using the dry biomass B_{TS}:

$$V_p = \frac{B_{TS}}{PDMC \cdot \rho_{Pf}} \tag{14}$$

where $PDMC$ is the ratio of plant dry mass to fresh mass and ρ_{Pf} is the fresh plant density. Table 1 provides some estimation for these parameters, as they were determined for selected plant groups near Trondheim (Norway) in July 2009. One has to have in mind that these parameters might change during the growing season. For most wetland plant communities dominated by grasses and sedges, the porosity is very high ($\varepsilon > 0.97$). In Mangrove swamps with dense networks of roots and pneumatophoras, ϕ reaches 0.10 to 0.45 (Mazda et al. 1997).

Table 1. Typical ranges for $PDMC$ and ρ_{Pf}.
n = Number of investigated species

Plant group	PDMC [kg/kg]	ρ_{Pf} [kg/m^3]
Ferns (n = 3)	0.15-0.20	800-900
Sedges (n = 3)	0.25-0.35	500-750
Grasses (*Poaceae*, n = 4)	0.35-0.45	500-750
Equisetum fluviatile	0.15-0.25	300-400
Aquatic species (n = 2*)	0.05-0.20	500-750

* *Potamogeton natans*, *Sparganium emersum*.

For the determination of the dynamic specific surface area a_{vd}, the surface area actually presented by the plant to the flow a_P has to be related to the plant volume V_P. For vegetated flow with very high porosities, partial overlapping of particles (here, stems and leaves) is less important than in densely packed beds. a_P is therefore identical with the static surface area a_s of the particles in the control volume.

For stiff vegetation, the parameter a_P is closely related to the vegetation density a and to parameters which are commonly used in vegetation sciences, i.e. the leaf area index LAI (the one sided leaf area per unit ground area). The LAI includes traditionally only the leaf area or the amount of green surfaces which are present on stems, leaf parts, buds, fruits and even under the bark of branches, due to their closed relation to photosynthesis or interception (Krause 1977). For many grass or sedge cover wetlands, the LAI is expected to be an appropriate parameter to estimate a_P.

In practice, it has to be tested which plant surface parameters are the best representations for a_P, and whether some species-specific or vegetation-type-specific coefficients or functions k_a and k_{LAI} can be derived from empirical data or geometrical relationships:

$$a_{vd} = \frac{a_P}{V_P} = \frac{k_a \cdot a}{V_P} = \frac{k_{LAI} \cdot LAI_{\Delta z}}{V_P} \tag{15}$$

where $LAI_{\Delta z}$ is the one-sided leaf area per unit ground area within the vertical unit Δz.. For stiff cylinder-like vegetation, a_P equals the product of π and a. Another useful parameter to estimate a_P based on information about the biomass is the leaf area ratio LAR (the amount of leaf area per unit dry biomass). Species-specific values for LAR can be found in literature, for example in Poorter and Remkes (1990). Hereby leaf area is given as half of the total area, similar to the definition of the LAI.

The tortuosity T for the plant types can be estimated from the porosity and the geometrical structure, for example using Equation 7.

3 METHODS AND MATERIALS

The study is a data analysis based on data from literature about flume experiments and field studies with emergent flow conditions (i.e. flow through vegetation, no overtopping) and particularly natural vegetation. The focus was on natural wetland vegetation. Some studies about emergent flow in non-wetland grasses and some flume experiments where the vegetation was represented by wooden dowels with nature-like vegetation densities were also included. The review that has been done so far is not complete yet.

For all of the studies, the friction factor f_P and the pore Reynolds number Re_P according to Equation 8 and 9 were determined. The pressure gradient was calculated from the water level or bed slope S, depending on the information available in the studies ($\Delta P/H = \rho g S$). The flow velocity U_0 was the discharge divided by the product of flow depth and width. The tortuosity T was computed using Equation 7 and ranged between 1.0 and 2.0. For cylindrical stems, all parameters were derived from the geometry. In the case of natural vegetation, if neither the porosity ε nor the plant volume V_P or the biomass B_{TS} was given, ε was set to 0.99. If the stem diameter d and the stem number m were the only available parameters to compute

the plant area, a_P and ε were calculated as for stiff cylinders and assumed to be constant over the inundated height. For the data by Chen (1976), the vegetation parameters were determined based on estimated values for the biomass and *LAI,* see Chapter 4. Tanino and Nepf's (2008) data was analyzed by applying the published regression coefficients and relations for the upper and lower value of the given *Re*-ranges.

In all cases, the vegetation was assumed to form a stiff porous medium with negligible effects of bending and streamlining, since the flow velocities were very low.

4 RESULTS AND DISCUSSION

4.1 *Pore friction coefficients*

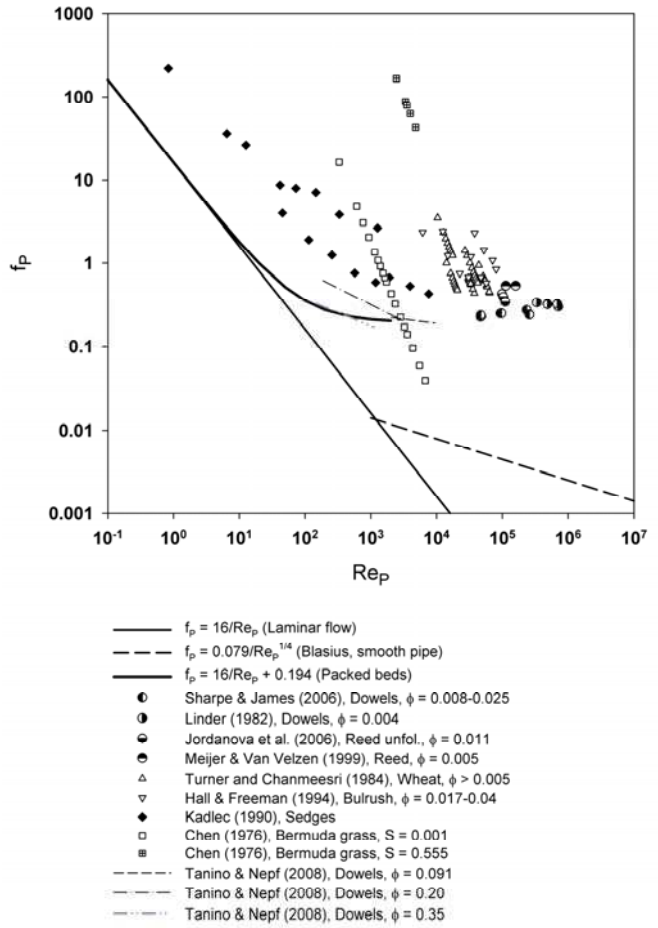

Figure 1. Calculated pore friction coefficients f_P versus pore Reynolds number Re_P for data from several studies (ϕ = solid volume fraction, S = slope).

In Figure 1, the calculated pore friction coefficients are plotted versus the pore Reynolds number (Moody chart). The straight lines are graphical representations for the laminar flow in pipes ($f_P = 16/Re_P$) and for turbulent flow in smooth pipes ($f_P = 0.079/Re_P^{1/4}$, Blasius) according to Douglas et al. (2005). The line for packed beds according to Comiti et al. (2000) is also included.

There is an apparent scatter, but most of the data points of the investigated data sets are concentrated along a zone above the packed bed curve by Comiti et al. (2000). Almost all of the studies were performed for very high nature-like porosities, with a solid fraction ϕ of less than 0.05. Only Tanino and Nepf (2008) worked with wooden dowels and solid fractions up to 0.35. The dashed lines show the range of their data, all of which was very close to the packed bed curve. In fact, their curve for the highest ϕ coincides with the packed bed curve, illustrating that the packed bed curve is valid also for porous media consisting of dense cylindrical arrays. Koch and Ladd (1997) investigated flows in random arrays of aligned cylinders. They showed that the theory for concentrated arrays, when the solid volume fraction is near the close packing limit, gave reasonable results for solid fractions larger than 0.30 to 0.40.

However, the data sets by Turner and Chanmeesri (1984) for wheat, Hall and Freeman (1994) for bulrush (*Scirpus validus*) and especially Chen (1976) for Bermuda grass (*Cynodon ssp.*) seem not to follow the described trend, but are arranged in line-like patterns in the logarithmic chart. For these data, ε and a_P were computed from the given stem diameter and stem number or from estimated biomass and *LAI*. ε and a_P were assumed to be constant over the height, since no other information was available. Some of the authors, however, mentioned that this was not true. Turner and Chanmeesri (1984) noted that the vegetation index they used did not take into account hairs on the stems nor the presence of dead leaves. The latter "were present in greater numbers for the higher stem densities, and possibly caused more drag than the stems" (p. 382).

In Figure 1, only the Bermuda grass series for the lowest (S = 0.001) and the highest bed slopes (S = 0.555) from Chen's (1976) comprehensive experimental series are shown. The data points for the other experiments with Bermuda grass arranged in a similar pattern in between, and Chen's data for Kentucky Blue grass (*Poa pratensis*) on the corresponding slopes did not differ very much from Bermuda grass. Since this data set shows the highest deviations from the generally observed pattern, it will be investigated more deeply in the following section.

4.2 *The importance of vertical structure for Bermuda grass*

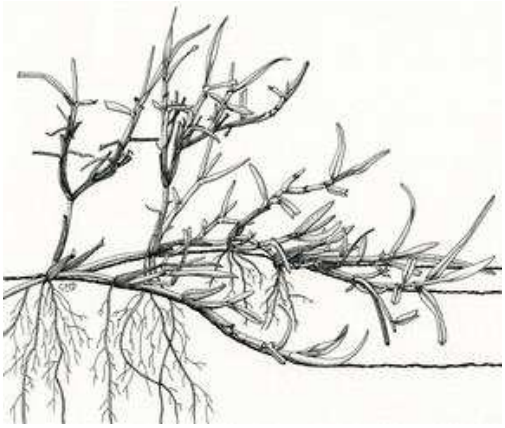

Figure 2. Overall plant structure of Bermuda grass (*Cynodon ssp*.). Courtesy by UC-IPM (2010).

For the Bermuda grass in Chen's (1976) experiments, the only available information about the vegetation was the species type, the average turf height (76 mm) and the description as "solid dense turf". Bermuda grass originally came from the savannas of Africa and is the common name for all the East African species of *Cynodon.* It is a plant that is grown as a turf grass or forage for livestock, but it also can be an invasive weed (UC-IPM 2010). Many hybrids have been developed specifically for use as turf grass. The species used by Chen (1976) was also a hybrid.

Bermuda grass (Fig. 2) is a creeping grass forming a dense mat on the ground. Its blades are short, usually 3 to 10 cm long with rough edges. The seed head stems can grow 10 to 40 cm tall. Compared with common Bermuda (*Cynodon dactylon*), the hybrids have greater turf density and fewer seed heads. They produce no viable seed and must be planted by vegetative means.

The dry biomass yield of Bermuda grass ranges between 200 and more than 900 g/m^2, depending on nutrient status and location (Kiniry et al. 2007). Burns and Fisher (2008) found average biomasses of 236, 408 and 525 g/m^2 for maintained canopy heights of 5.6 cm, 10.1 cm and 13.1 cm, respectively, in the southeastern USA. The average seasonal maximum of the *LAI* for coastal bermuda grass was estimated with 2.2 by Kiniry et al. (2007) for diverse sites in Texas (USA) with a mean aboveground dry biomass production of 630 g/m^2. The seasonal maximum *LAI* values of their measurements ranged between 1.2 and 5.5.

Chen (1976) used sodded turfs for his experiments. Based on the above mentioned values and assuming a low to mean nutrient status, it seems reliable to assume a biomass B_{TS} in the range of 200 to 400 g/m^2 for the 7.6 cm tall turfs. The *LAI* is estimated to range between 1 and 3. The values for the computations shown in Fig. 1 and 4 were B_{TS} = 300 g/m^2, $PDMC$ = 0.4, ρ_{Pf} = 700 kg/m^3 and LAI = 2. The *LAI* was used to compute the plant area a_P, leading to $k_{LAI} \cdot LAI_{\Delta z}$ = 2·(2/0.076 m) = 52.6 m^{-1}. For the computation shown in Figure 1, this value was taken as constant over the entire vegetation height for Chen's data.

Looking at Figure 2, it is easy to recognize that this assumption oversimplifies the real plant structure. Most grassland has vegetation structure profiles where both B_{TS} and *LAI* decrease with height (Heil 1988, Dierschke 1994). For tall wetland communities, the lower part of the canopy that comprises mainly stems can be greater in mass, but occupy less flow area, such that the *LAI* profile has a maximum at some height above the ground and differs from that of the biomass B_{TS} (Hirose and Werger 1995).

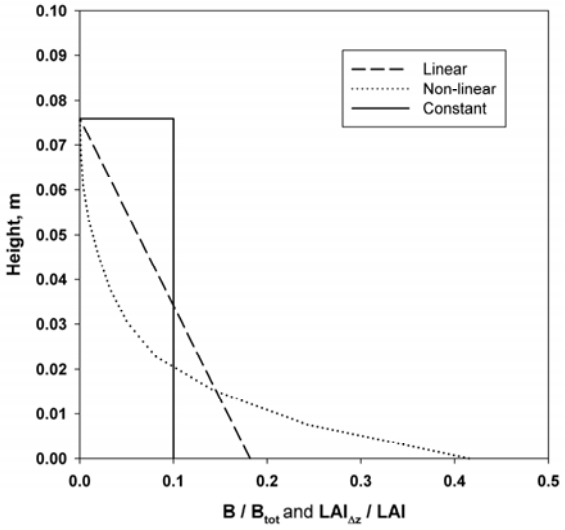

Figure 3. Vertical structure profiles used for the calculations. B_{tot} is the total dry biomass per unit ground area.

To investigate the effect of vertical canopy structure on the computed pore friction coefficients for Chen's (1976) data for Bermuda grass, the values were calculated using a linear and a non-linear structure profile, as illustrated in Figure 3. In the non-linear profile, most of the biomass is concentrated in the lowest layer closest to the ground. For simplification, the same vertical distribution for biomass and leaf area was assumed.

Figure 4 shows the results in comparison with the calculated values for a constant distribution over the vertical. For the "layer-averaged values", the porosity ε and the area a_P were computed as averages over the inundated vegetation height for the given water depth. For the "topmost-layer values", the values of the topmost inundated layer were used instead. On the first view, it seems more reliable to work with the "layer-averaged

values". However, this does not correspond to the real flow process in the Bermuda grass layer, which is most likely non-linear stratified. Here the available flow area and the number of flow-dominating macro-pores may increase much more rapidly than linearly with increasing flow depth, such that most of the flow goes through the most permeable topmost layer (Busch et al. 1993).

Figure 4 illustrates that both the type of vertical structure profile and the method of calculation for ε and a_P affect the calculated pore friction coefficients. For the calculation with depth-averaged values, the pattern of the f_P-versus-Re_P-relation for Bermuda grass changes only slightly both for the linear and non-linear profile. For the non-linear profile, the results are highly depending on the averaging method.

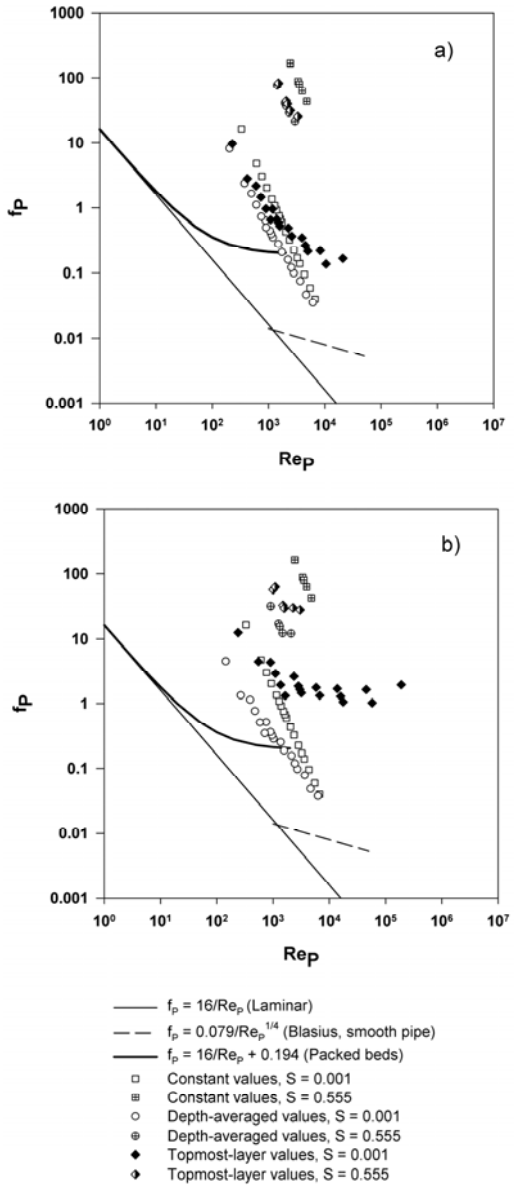

Figure 4. Calculated pore friction coefficients for Chen's (1976) data for Bermuda grass, a) for the linear vertical profile and b) for the non-linear vertical profile.

Using the depth-averaged values for ε and a_P, the calculated pore friction coefficients aligned more or less parallel to the laminar flow line. Applying the topmost-layer values, the data points for the lower slopes fell within the range of the other investigated data above the packed bed curve by Comiti et al. (2000). The real values are expected to range between those computed using the depth-averaged values and those computed using the topmost-layer values for the non-linear profile, eventually with deviations because of the crude estimations for B_{TS} and a_{vd}.

The investigation showed that the pattern of the computed f_P-versus-Re_P-relation for Bermuda grass is highly influenced by the assumptions about the vertical structure of the grass layer. The use of more realistic vertical biomass and plant area profiles together with an averaging method that accounts for the real change in flow velocity with increasing depth might lead to an f_P-versus-Re_P-relation for Bermuda grass which is comparable to that for the other investigated data sets. Similar corrections could possibly be done for the data of Turner and Chanmeesri (1984) for wheat and Hall and Freeman (1994) for bulrush.

The results were in agreement with James et al. (2008) who argued that the variation of C_D with Re_d for natural emergent vegetation was a result of the combined effect of vertical foliage density variation and foliage flexibility. The effect of flexibility was not taken into account in this study and might be a reason for the some scatter of the data. Especially for the high-slope experiments, the flow velocity in the vegetated layer might have been large enough to cause some deflections of the smallest leaves or plant hairs.

4.3 *Vertical structure for the sedge type*

The influence of the vertical structure can be further illustrated for sedges (*Carex spec*.) which are typical for wetlands. Kadlec (1990) measured vegetation-density profiles for the sedge cover type at Houghton Lake (Michigan, USA). He determined the frontal area per volume and the leaf size. He found a large frontal area in the litter layer (the lowest 5 cm), which decreased to zero at the top of the canopy (Figure 5a). Leaves were thicker near their base, but litter contained fragments of all sizes.

His data allowed the calculation of vertical profiles for the number of leaves and the spacing s between the leaves. Because of the internal structure of the plants, the number of leaves and the spacing between the leaves were almost constant above the litter layer, despite the large decrease in frontal area a over the height. The vertical profile for s^2 is shown in Figure 5b. The calculated values for s^2 correspond remarkably well with the permeability profile which was derived using Equation 3

from the filtration coefficients measured by Ivanov (1975) for the *Carex-Hypnum* vegetation type in Russia (*Hypnum* = a moss genus). His filtration coefficients were measured using large undisturbed samples that were cut in the frozen state and transferred into the laboratory. The absolute values of the permeability for Ivanov's *Carex-Hypnum* type were lower than those for Kadlec's sedge cover type, but the vertical profiles were similar because of the sedge-typical vertical structure of the vegetation.

The almost constant values for the leaf spacing over the vertical, together with a decreasing projected area, have consequences for the flow and turbulence structure within the vegetation. In the upper layers, the drag exerted by the vegetation is relatively low because of the decreased projected area, but the integral length scale for turbulent motions is still restricted by the relatively small spacing values between the leaves.

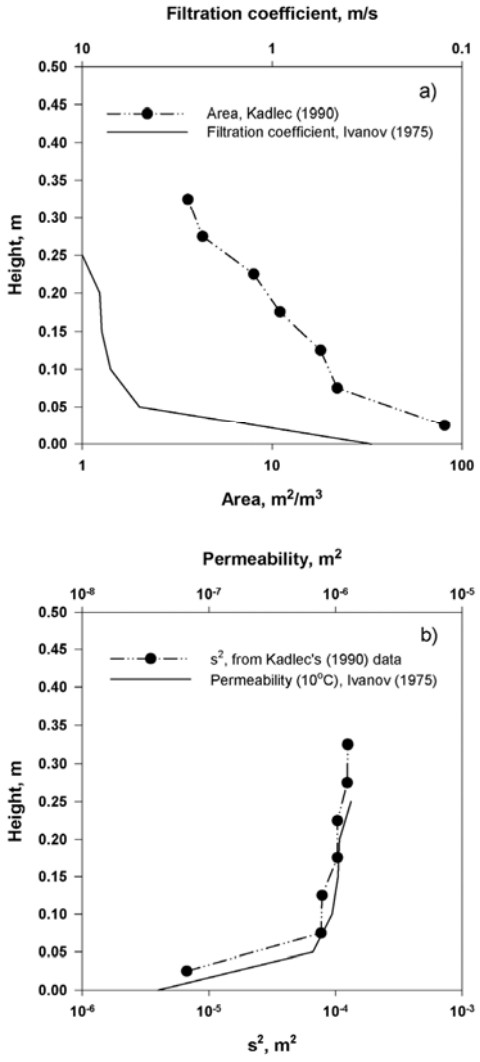

Figure 5. Vertical profiles for the sedge type, a) frontal area according to Kadlec (1990) and filtration coefficient according to Ivanov (1975) b) calculated values for s^2 and permeability.

Therefore the vegetation seems to have a turbulence-damping effect, suppressing the onset of larger fluctuations. A similar "laminarising" effect was observed for reticulated media by Seguin et al. (1998). Schnauder et al. (2007) found reduced turbulence intensity in the wake behind a permeable plant, compared to a non-permeable counterpart.

5 CONCLUSIONS

Methods from porous flow were adapted to compute the pore friction coefficient f_P and the pore Reynolds number Re_P for emergent natural vegetation based on criteria such as biomass and *LAI*. The calculated relations between f_P and Re_P for several flume and field data sets from literature were shown in a Moody chart. There was an apparent scatter, but most of the data points were concentrated within a belt above the packed bed curve of Comiti et al. (2000).

At present it is unclear whether there is a universal law for flow resistance of emergent wetland vegetation with a tendency to range within this belt. It is possible that the chart (Figure 1) has to be completed with a series of lines similar to the classical Moody chart, since the high-slope experiments from Chen (1976) led to a higher pore friction coefficient than the other data points. It has to be noted, however, that some of his experiments were performed using extremely high slopes which are very unlikely to occur under natural conditions.

It was illustrated that the vertical structure of the vegetation plays an important role for the characteristic of flow resistance. For the sedge type it was shown that the projected area *a* changed significantly with height, but the values for the leaf spacing *s* did not. This is assumed to affect turbulence and to have a "laminarising" effect on the flow inside the vegetation. The natural plant structure is therefore a key factor for the understanding of vegetation flow resistance.

The study showed that the flow resistance of natural wetland vegetation can be described and compared based on parameters like biomass and *LAI* together with a porous media model. However, the uncertainties about some parameters, and especially about the vertical structure of the vegetation in the investigated data sets, did not allow a final assessment of the proposed method. Furthermore, the study is based on a limited number of data sets so far. More and better measurement data has to be acquired and included to test and develop the approach.

REFERENCES

Breugem, W. P. 2004. The influence of wall permeability on laminar and turbulent flows. PhD thesis, Delft University of Technology.

Burns J. C., Fisher, D. S. 2008. "Coastal" and "Trifton 44" bermudagrass availability on animal and pasture productivity. Agronomy Journal 100 (5), 1280-1288.

Busch, K. F., Luckner, L., Tiemer, K. 1993. Geohydraulik. Gebrüder Bornträger Berlin.

Chen, C. 1976. Flow Resistance in Broad Shallow Grassed Channels. ASCE Journal of the Hydraulics Division 102(HY3), 307-322.

Comiti, J., Renaud, M. 1989. A new model for determining mean structure parameters of fixed beds from pressure drop measurements: Application to beds packed with parallelepipedal particles. Chemical Engineering Science 44(7), 1539-1545.

Comiti, J., Sabiri, N.E., Montillet, A. 2000. Experimental characterization of flow regimes in various porous media – III: limit of Darcy's or creeping flow for Newtonian and purely viscous non-Newtonian fluids. Chemical Engineering Science 55, 3057-3061.

Diedericks G. P. J., Du Plessis, J. P. 1997. Modelling of flow through homogenous foams. Math. Engng. Ind. 6(2), 133-154.

Dierschke, H. 1994. Pflanzensoziologie. Ulmer, Stuttgart.

Douglas J. F., Gasiorek, J. M., Swaffield J. A., Jack, L. B. 2005. Fluid mechanics. 5. Edition. Pearson Education, London.

Hall B. R., Freeman, G. E. 1994. Study of hydraulic roughness in wetland vegetation takes new look on Manning's n. The Wetland Research Program Bulletin 4(1), 1-4.

Heil, G. 1988. LAI of grasslands and their roughness length. In: Verhoeven J. T. A. and Werger J. M. A. (eds.) Vegetation structure in relation to carbon and nutrient economy, SPB Academic Publishing The Hague, 149-155.

Hirose, T., Werger, M. J. A. 1995. Canopy structure and photon flux partitioning among species in a herbaceous plant community. Ecology 76(2), 466-474.

Hoffmann, M. R. 2004. Application of a Simple Space-Time Averaged Porous Media Model to Flow in Densely Vegetated Channels. Journal of Porous Media 7(3), 183-191.

Ivanov, K. E. 1975. Vodoobmen v bolotnyh landšaftah. Leningrad, Gidrometeoizdat.

James, C. S., Goldbeck, U. K., Patini, A., Jordanova, A. A. 2008. Influence of foliage on flow resistance of emergent vegetation. Journal of Hydraulic Research 46(4), 536-542.

Jordanova A. A., James, C. S., Birkhead, A. L. 2006. Practical estimation of flow resistance through emergent vegetation. Water Management 159(3), 173-181.

Kadlec, R. H. 1990. Overland Flow in Wetlands: Vegetation Resistance. J Hydr Engin ASCE 116(5), 691-706.

Koch, D. L., Ladd, A. J. C. 1997. Moderate Reynolds number flows through periodic and random arrays of aligned cylinders. J. Fluid Mech. 349, 31-66.

Krause, W. 1977. Application of vegetation science to grassland husbandry. In: Tüxen, R. (ed.) Handbook of vegetation science. Dr. W. Junk b. v. Publishers, The Hague.

Kiriny, J. R., Burson, B. L., Evers, G. W., Williams, J. R., Sanchez, H., Wade, C., Featherston, J. W., Greenwade, J. 2007. Coastal Bermudagrass, Bahiagrass, and Native Range Simulation at Diverse Sites in Texas. Agron. J. 99, 450-461; DOI: 10.2134/agronj2006.01119.

Lindner, K. 1982. Der Strömungswiderstand von Pflanzenbeständen. Leichtweiss-Institut für Wasserbau der Technischen Universität Braunschweig, Mitteilungen 75/1982.

Mazda, Y., Wolanski, E., King, B., Sase, A., Ohtsuka, D., Magi, M. 1997. Drag force due to vegetation in mangrove swamps. Mangroves and Salt Marshes 1, 193-199.

Meijer D. G., Van Velzen, E. H. 1999. Prototype-scale flume experiments on hydraulic roughness of submerged vegetation. Proceedings of the 28th International IAHR Conference, Graz, Austria.

Nepf, H., 1999. Drag, turbulence, and diffusion in flow through emergent vegetation. Water Resources Research 35(2), 479-489.

Poorter, H., Remkes, C. 1990. Leaf area ratio and net assimilation rate of 24 wild species differing in relative growth rate. Oecologia 83, 553-559.

Schnauder, I., Yagci, O., Kabdasli, S. 2007. The effect of permeability of natural emergent vegetation on flow velocities and turbulence. Proceedings of the 32nd IAHR Congress, Venice, Italy.

Seguin, D., Montillet, A., Comiti, J. 1998. Experimental characterization of flow regimes in various porous media-I: Limit of laminar flow regime. Chemical Engineering Science 53(21), 3751-3761.

Serra, T., Fernando, H. J. S., Rodriguez, R. V. 2004. Effects of emergent vegetation on lateral diffusion in wetlands. Water Research 38, 139-147.

Sharpe, R. G., James C. S. 2006. Deposition of sediment from suspension in emergent vegetation. Water SA 32(2), 211-218.

Tanino, Y., Nepf, H. 2008. Laboratory Investigation of Mean Drag in a Random Array of Rigid, Emergent Cylinders. Journal of Hydraulic Engineering ASCE 134(1), 34-39. DOI: 10.1061(ASCE)0733-9429(2008)134:1(34).

Tsihrintzis V. A., Madiedo, E. E. 2000. Hydraulic Resistance Determination in Marsh Wetlands. Water Resources Management 14, 285-309.

Turner A. K., Chanmeesri, N. 1984. Shallow flow of water through non-submerged vegetation. Agricultural Water Management 8(4), 375-385.

UC-IPM 2010. How to Manage Pests. The UC Guide to Healthy Lawns. Accessed 30. January 2010 (http://www.ipm.ucdavis.edu/TOOLS/TURF/TURFSPECIES/bermuda.html).

Whitaker, S. 1996. The Forchheimer equation: a theoretical development. Transport in Porous Media 25, 27-61.